Volume 61
Number 52
4 July 2025
Pages 9331–9518

ChemComm

Chemical Communications

rsc.li/chemcomm

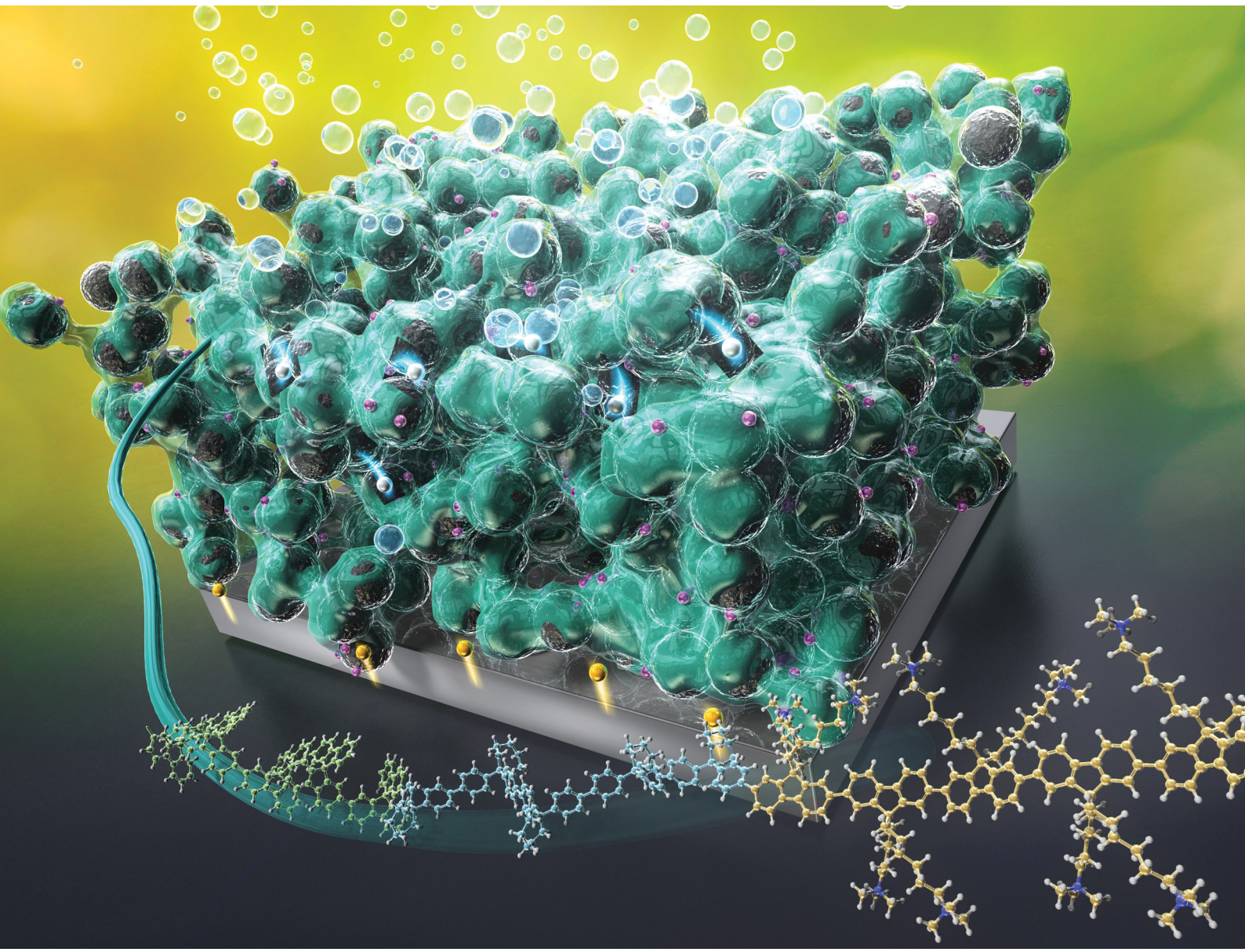

ISSN 1359-7345

ROYAL SOCIETY OF CHEMISTRY

COMMUNICATION

Kenji Miyatake *et al.*

Boosting the hydrogen evolution reaction catalytic activity of Pt/C *via* well-designed anion-exchange ionomers

ChemComm

COMMUNICATION

View Article Online
View Journal | View Issue

Cite this: *Chem. Commun.*, 2025, **61**, 9412

Received 4th April 2025,
Accepted 8th May 2025

DOI: 10.1039/d5cc01899d

rsc.li/chemcomm

Boosting the hydrogen evolution reaction catalytic activity of Pt/C *via* well-designed anion-exchange ionomers†

Fang Xian,[a] Kenji Miyatake,*[abc] Lin Guo,[a] Guoyu Shi,[b] Fanghua Liu,[a] Ahmed Mohamed Ahmed Mahmoud,[a] Vikrant Yadav[a] and Chun Yik Wong[a]

Ionomer binders are highly important for maximizing the performance of nanoparticle catalysts, yet their development has received limited attention. In this study, novel fluorine-free anion-exchange copolymer and terpolymer-based ionomers containing cyclic and rigid structures were designed to enhance ion conductivity and free volume, thereby promoting rapid mass transport and improved reaction kinetics for the alkaline HER.

Hydrogen energy is critical to achieving a carbon-neutral society, in which water electrolysis is expected to play a pivotal role in producing green hydrogen for renewable energy.[1,2] Compared to alkaline water electrolysis (AWE) and proton exchange membrane water electrolysis (PEMWE), which have already been commercialized, anion-exchange membrane water electrolysis (AEMWE) shows more promise in terms of energy conversion and cost efficiency.[3,4] The challenges in AEMWE include developing better functioning AEMs and cathode catalysts. Although substantial effort has been devoted to nonplatinum (Pt) group metal-based cathode catalysts, Pt is still a benchmark catalyst for the hydrogen evolution reaction (HER) because of its fast reaction kinetics. Nevertheless, its activity is ~2 orders of magnitude lower in alkaline media than in acidic conditions because of the water dissociation step required for hydrogen evolution.[5] Although previous research on the electrocatalytic HER in alkaline conditions has focused on catalysts, ionomer binders are also important in catalyst layers where the catalysts, ionomer electrolytes, and liquid water must cooperate.[6]

Recent progress in AEMs is impressive, particularly in terms of ion conductivity and alkaline stability.[7,8] However, few studies have explicitly explored the role of ionomer binders and their optimization.[6,9] Well-designed binders must have high ion conductivity and alkaline stability, as well as homogeneous catalyst dispersion and efficient mass transport (ion transport and gas diffusion).[10] Nafion, a perfluorinated sulfonic acid polymer, is a benchmark proton conducting ionomer that has been widely used as a binder in rotating disk electrode measurements for high pH electrochemical studies. However, it is unsuitable for accurate electrochemical kinetic measurements because of its poor hydroxide ion (OH^-) conductivity in alkaline environments.[11] Therefore, the effect of binders on catalytic activity has not been well investigated, and the same anionic conducting polymers employed as AEMs are utilized in the binders in practical AEMWEs.[12,13]

We have previously developed a series of aromatic polymer-based AEMs. The QPAF-4 membrane with a perfluoroalkylene backbone and pendant ammonium groups, for example, demonstrated high OH^- conductivity, excellent mechanical properties, and alkaline stability, achieving a current density of ~1.0 A cm^{-2} at a low cell voltage of 1.71 V after a 1000-hour durability test.[14,15] Tanaka *et al.*[16] investigated the effect of QPAF-4 ionomers with different ion-exchange groups (trimethylammonium, ethyldimethylammonium, and piperidinium) on the HER/hydrogen oxidation reaction (HOR) of Pt (110). Their results showed that the QPAF-4 ionomer with more hydrophilic ion-exchange groups (trimethylammonium) increased the HER/HOR activity.[16] More recently, highly gas-permeable ion-exchange ionomers, QC6xBA (anionic) and SBAFC6 (protonic), were designed by introducing bulky cyclohexyl (C6) groups into the polymer backbones, which demonstrated hydrogen and oxygen permeability exceeding that of the benchmark Nafion ionomer, resulting in high AEMWE and PEMFC performance.[17,18]

The high cost and environmental persistence of those partially fluorinated ionomers, however, have highlighted the need for innovative fluorine-free alternatives.[19,20] In the present study, inspired by the function of C6 in the ionomers and the effect of the pendant ammonium group of QPAF-4 on the HER/HOR of Pt (110), bulky cycloheptane (C7) was designed to combine the hydrophilic fluorenyl

[a] *Clean Energy Research Center, University of Yamanashi, Kofu, Yamanashi 400-8510, Japan. E-mail: miyatake@yamanashi.ac.jp*
[b] *Hydrogen and Fuel Cell Nanomaterials Center, University of Yamanashi, Kofu, Yamanashi 400-8510, Japan*
[c] *Department of Applied Chemistry, Waseda University, Tokyo 169-8555, Japan*

† Electronic supplementary information (ESI) available: Experimental procedures, characterisation for new ionomers including NMR spectra, BET and HER. See DOI: https://doi.org/10.1039/d5cc01899d

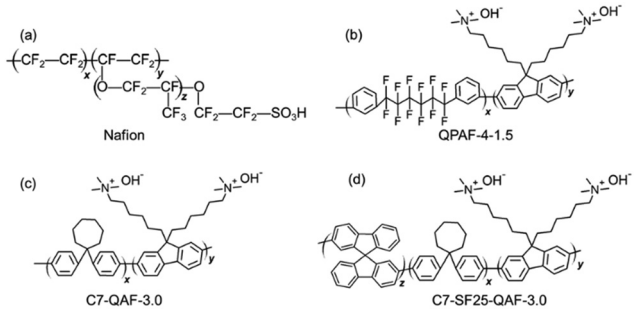

Fig. 1 Structures of different ionomers: (a) Nafion, (b) QPAF-4-1.5, (c) C7-QAF-3.0 and (d) C7-SF25-QAF-3.0.

scaffold with pendant ammonium groups for a new anion conductive binder (C7-QAF). Furthermore, 9,9′-spirobi[9*H*-fluorene] (BSF) with a rigid backbone was introduced to produce a large free volume in the membranes and facilitate mass transport. Compared to QPAF-4,[14] which exhibited high swelling at an ion-exchange capacity (IEC) >2 mequiv. g^{-1}, the C7-QAF and C7-SF25-QAF membranes with a higher IEC of 3.0 mequiv. g^{-1} maintained smaller dimensional changes while enabling high ion conductivity. The C7-QAF and C7-SF25-QAF ionomers were evaluated as binders for Pt/C catalysts in the HER.

Fig. 1 presents the structural characteristics of different ionomer binders, including a benchmark proton exchange membrane (Nafion) and a series of anion-exchange ionomers. Our original AEM, QPAF-4, with an IEC of 1.5 mequiv. g^{-1} was synthesized according to our previous report.[14] The successful synthesis of QPAF-4-1.5 was confirmed using proton nuclear magnetic resonance (^{1}H NMR) spectroscopy (Fig. S1, ESI†). To develop fluorine-free AEM, a hydrophobic monomer with a bulky C7 group was synthesized *via* acid-catalyzed condensation and Sandmeyer reactions (Scheme S1 and Fig. S2, ESI†). Substituting perfluorohexylene biphenylene, a copolymer containing hydrophobic C7 and hydrophilic fluorenyl groups with pendant ammonium groups, was synthesized and quaternized (Fig. S3, ESI†). Furthermore, a terpolymer with a bridged polycyclic compound (BSF, synthesized as shown in Scheme S2 and Fig. S4, ESI†) as another hydrophobic component was synthesized with a BSF to C7 molar ratio of 1 : 3. The ^{1}H spectrum (Fig. S5, ESI†) confirmed the theoretical chemical structure of C7-SF25-QAF. The molecular weight of the polymer increased slightly with the addition of the BSF monomer (Table S1, ESI†). The target IEC of the quaternized copolymer (C7-QAF) and terpolymer (C7-SF25-QAF) was set at 3.0 mequiv. g^{-1}, expecting high ion conductivity. All quaternized polymers exhibited good solubility not only in highly polar solvents such as *N*,*N*-dimethylacetamide and dimethyl sulfoxide but also in lower alcohols such as methanol, which is highly beneficial for the preparation of catalyst inks and for cleaner catalyst layers with less chance of residual solvent contamination. All polymers formed transparent and bendable membranes after solution casting.

The water uptake and dimensional changes of Nafion and a series of anionic ionomer membranes were investigated (Fig. 2a). Water uptake (at room temperature) was mostly dominated by the IEC value, with the Nafion membrane showing the lowest water uptake. Compared to the C7-QAF-3.0 membranes, the C7-SF25-QAF-3.0 terpolymer membranes displayed higher water uptake because of the higher titrated IEC. The swelling ratio was less dependent on the IEC. Compared to the Nafion and QPAF-4-1.5 membranes, the fluorine-free C7-QAF-3.0 and C7-SF25-QAF-3.0 membranes exhibited smaller dimensional changes despite their higher IEC. Furthermore, the dimensional changes were less dependent on temperature for the C7-QAF-3.0 and C7-SF25-QAF-3.0 membranes, presumably because of the rigid aromatic moieties of the C7 and BSF hydrophobic components, providing the potential advantage of long-term durability in water electrolysis cells.

The proton (H^+) conductivity of Nafion and OH^- conductivity of the anionic ionomer membranes were measured in degassed water at different temperatures from 30 °C to 80 °C (Fig. 2b). The Nafion membranes exhibited high H^+ conductivity (197.7 mS cm^{-1} at 80 °C), which was largely attributed to their well-developed phase-separated morphology with interconnected ionic channels, in which protons migrate *via* the Grotthuss mechanism.[21] For AEMs, similar to water uptake, the OH^- conductivity increased with increasing IEC because water molecules also promoted ion transport. The C7-SF25-QAF-3.0 membranes exhibited the highest OH^- conductivity (196.3 mS cm^{-1} at 80 °C), which was comparable to that of Nafion and higher than that of the reported QPAF-4-3.0 (140 mS cm^{-1} at 80 °C),[15] C7-QAF-3.0 (165.8 mS cm^{-1}), and QPAF-4-1.5 (86.9 mS cm^{-1}). These results suggest that hydrophobic BSF considerably increased OH^- conduction in the membranes. Ionomer binders with high ionic conductivity are beneficial in rapidly delivering ions to the catalyst surface for efficient electrochemical reactions.

Brunauer–Emmett–Teller (BET) analysis was performed on the different ionomer binders (Fig. S6, ESI†) and the results are summarized in Table S2, ESI.† Compared to Nafion (6.89 m^2 g^{-1}), the QPAF-4-1.5 and C7-QAF-3.0 ionomers exhibited lower BET surface areas (<3 m^2 g^{-1}), with all three ionomers possessing low pore volumes (<0.02 cm^3 g^{-1}). In contrast, the C7-SF25-QAF-3.0 polymer demonstrated a much higher surface area (15.36 m^2 g^{-1}) and larger pore volume (0.29 cm^3 g^{-1}), probably because of the greater free volume generated by the rigid nature of the BSF component, which in turn might potentially promote mass transport to the catalyst surface.[22,23] Fig. S7 (ESI†) presents the pore size distribution of the ionomers between 0–20 nm. Nafion, QPAF-4-1.5, and

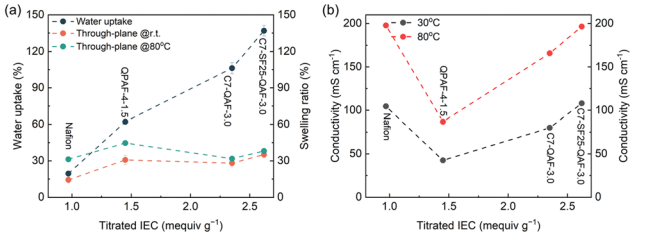

Fig. 2 (a) Water uptake and through-plane swelling at 25 °C and 80 °C and (b) ionic conductivity of Nafion and a series of anionic ionomer membranes as a function of titrated IEC.

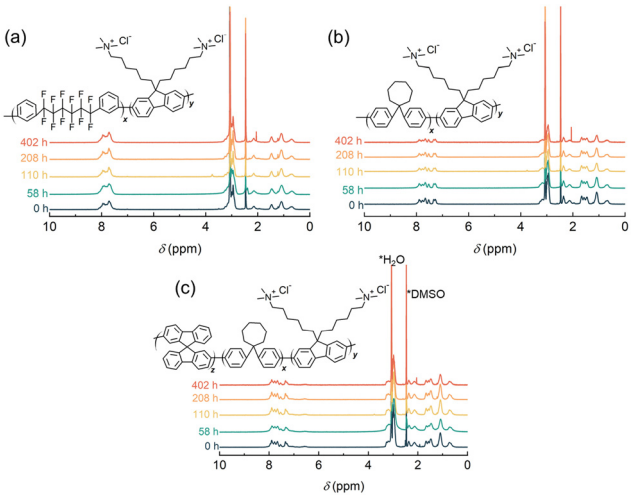

Fig. 3 ^{1}H NMR spectra of the (a) QPAF-4-1.5, (b) C7-QAF-3.0, and (c) C7-SF25-QAF-3.0 ionomer membranes after treatment with 4 M KOH at 80 °C for different times.

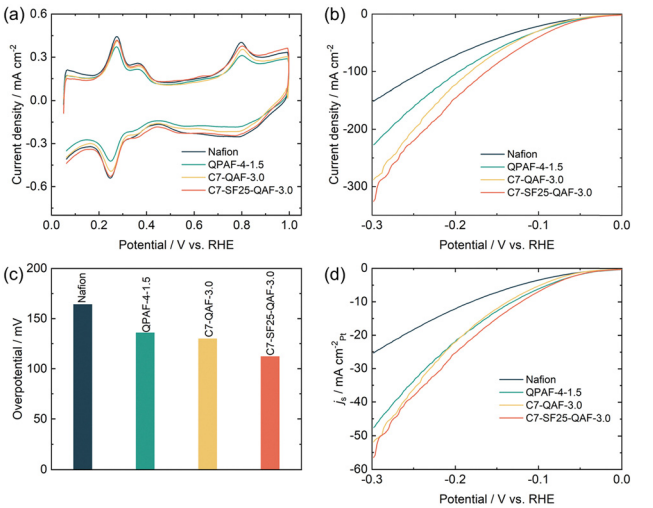

Fig. 4 (a) Cyclic voltammograms (CVs) of the Pt/C catalyst covered with different ionomer binders in 1 M KOH at 50 mV s^{-1}. (b) Linear sweep voltammograms (LSVs) of the Pt/C catalyst covered with different ionomer binders in 1 M KOH at 10 mV s^{-1} and 3000 rpm. (c) HER overpotential at −50 mA cm^{-2}. (d) LSVs of the Pt/C catalyst covered with different ionomer binders normalized with Pt surface area.

C7-QAF-3.0 exhibited sharp and intense peaks at 3–5 nm, whereas C7-SF25-QAF-3.0 ionomer showed a broader peak ranging from 3–15 nm with comparable intensity, suggesting a broader pore size distribution and potential pore connectivity. This would contribute to the formation of an ionic network, thereby improving ionic conduction and catalyst utilization.[24]

The alkaline stability of the ionomer membranes was tested in harsh alkaline conditions (4 M KOH at 80 °C), with the chemical structural changes monitored using ^{1}H NMR. Similar to the pristine membranes, the alkali-treated anionic ionomers were soluble in deuterated dimethyl sulfoxide (DMSO-d_6). No additional peaks were observed in the ^{1}H NMR spectra of the post-test samples compared to the pristine ionomers (Fig. 3). In particular, the lack of peaks at 4–6 ppm (degradation products from Hoffmann elimination of the ammonium groups) and 1.8–2.0 ppm (degradation products from nucleophilic substitution of the ammonium groups) indicated the stability of the pendant ammonium groups.[14] The aromatic main chains were also intact. Table S3 (ESI†) compares the ion conductivity and alkaline stability of state-of-the-art fluorine-free AEMs.[8,9,25–27] The C7-SF25-QAF-3.0 membrane displayed amongst the highest OH^- conductivity and competitive alkaline stability under harsh conditions.

A suitable catalyst particle–binder combination is key to forming a homogeneous catalysis layer in the membrane electrode assembly to achieve high-performance AEMWEs. The effect of ionomer binders on the HER activity was evaluated in 1 M KOH. Fig. 4a shows the cyclic voltammograms (CVs) of Pt/C catalysts covered with different ionomer binders, in which typical hydrogen adsorption/desorption (H_{UPD}) peaks were observed below 0.5 V *vs.* a reversible hydrogen electrode (RHE). The electrochemically active surface area (ECSA) was calculated from the reduction peak of H_{UPD}, in which the QPAF-4-1.5 ionomer exhibited a lower ECSA value than the C7-QAF-3.0 and C7-SF25-QAF-3.0 ionomers, probably because of the greater hydrophobicity and lower IEC of QPAF-4-1.5 (Table S4, ESI†). Fig. 4b displays the linear sweep voltammograms (LSVs) (geometric current density) of the ionomer-covered Pt/C samples. The onset potential for the HER was ∼0 mV *vs.* RHE for all electrodes.

The HER catalytic activity was dependent on the covering ionomer. For quantitative discussion, the overpotential at −50 mA cm^{-2} was compared (Fig. 4c). Nafion-Pt/C exhibited the lowest HER activity with the highest overpotential (164 mV) because of its intrinsic H^+ (but not OH^-) conducting properties, resulting in sluggish HER kinetics in alkaline media.[11] In contrast, the overpotential with the anionic ionomers was much smaller by 28–52 mV. In particular, the Pt/C catalyst with the C7-SF25-QAF-3.0 ionomer achieved the lowest overpotential (112 mV), followed by the C7-QAF-3.0 (130 mV) and QPAF-4-1.5 (136 mV) ionomers. The catalytic activity of the anionic binder was in the same order as for the OH^- conductivity because high ionic conductivity promoted rapid OH^- transfer. Fig. 4d presents the LSVs with normalized current density by the ECSA of Pt to represent the intrinsic HER activity, denoted as specific activity (J_S).

The Pt/C catalysts with anionic ionomers displayed higher HER specific activities (*e.g.*, ∼1.5–2 times higher current density at −0.1 V) than that with the Nafion binder, and the C7-SF25-QAF-3.0 ionomer-Pt/C exhibited the highest specific activity (7.0 mA cm_{Pt}^{-2} at −0.1 V). The QPAF-4-1.5 ionomer-Pt/C sample showed a slightly higher HER specific activity than the C7-QAF-3.0 ionomer-Pt/C because of its lower ECSA value. Then, the Pt mass-based catalytic activity was compared (Fig. S8a, ESI†). C7-SF25-QAF-3.0 ionomer-Pt/C exhibited the highest activity (4.02 A mg_{Pt}^{-1} at −0.1 V), which was ∼1.9 times higher than that of the Nafion-Pt/C sample (2.10 A mg_{Pt}^{-1} at −0.1 V) and ∼1.4 times higher than those of the QPAF-4-1.5 (2.94 A mg_{Pt}^{-1} at −0.1 V) and C7-QAF-3.0 (2.93 A mg_{Pt}^{-1} at −0.1 V) samples (Fig. S8b, ESI†). This suggests improved Pt utilization resulting from the high BET surface area and sufficient porosity to facilitate ion transport and gas diffusion. The high mass activity enables lower Pt usage when applying the C7-SF25-QAF-3.0 ionomer binder in practical AEMWEs.

In addition, a semicommercial Tokuyama AS-4 anion-exchange binder was also evaluated as a reference. As shown in Fig. S9 (ESI†), the HER performance of the AS-4-Pt/C catalyst was comparable or slightly better than that of the QPAF-4-1.5 and C7-QAF-3.0 based systems. The C7-SF25-QAF-3.0 ionomer-Pt/C catalyst exhibited significantly enhanced activity with the lowest overpotential, a 1.17-fold increase in the specific activity, and a 1.22-fold increase in mass activity, highlighting the outstanding catalytic performance of this anionic ionomer.

The morphology of the ionomer-coated Pt/C catalyst was investigated by transmission electron microscopy (TEM, Fig. S10, ESI†). In the C7-SF25-QAF-3.0-Pt/C system, the catalyst surface was uniformly covered with a thin ionomer layer ($\sim$2 nm, yellow dashed line), indicating good interfacial compatibility. This conformal coating would account for the superior catalytic performance by promoting effective catalyst-ionomer interaction and reactant accessibility. In contrast, QPAF-4-1.5 and AS-4 binders were less uniform with an inhomogeneous layer. Scanning electron microscopy (SEM) images further revealed pronounced ionomer agglomerates in the QPAF-4-1.5 and AS-4 based systems, whereas the C7-SF25-QAF-3.0-Pt/C ink displayed a well-dispersed morphology uniformly covering the Pt/C catalyst (Fig. S11, ESI†). These results reveal a clear correlation between the ionomer binder structure and the HER performance of Pt/C. A bent and porous backbone would be more compatible with Pt/C than the linear perfluorinated systems, which enabled more uniform coverage on Pt/C, facilitated fast ion-transport, avoided excessive blockage of Pt active sites, and thereby improved the catalytic performance.

In summary, two novel fluorine-free copolymer (C7-QAF) and terpolymer (C7-SF25-QAF)-based anion-exchange ionomers comprising C7 groups and a hydrophilic fluorenyl scaffold with pendant ammonium groups were successfully designed and synthesized as binders for modified Pt/C electrodes. With a high IEC of 3.0 mequiv. g^{-1}, both ionomers displayed small dimensional changes at 80 °C, as well as good solubility in high boiling point solvents and lower alcohols. The C7-SF25-QAF-3.0 terpolymer exhibited OH^- conductivity (196.3 mS cm^{-1} at 80 °C) that was higher than that of C7-QAF-3.0 (165.8 mS cm^{-1} at 80 °C) and comparable to the H^+ conductivity of the benchmark proton exchange Nafion membrane. In addition, the inclusion of rigid BSF created more free volume in the C7-SF25-QAF-3.0 ionomer, providing a large BET surface area (15.36 m^2 g^{-1}) and pore volume (0.29 cm^3 g^{-1}). This in turn promoted good mass transport capability to the catalyst surface. As a result, the Pt/C covered with the C7-SF25-QAF-3.0 binder demonstrated the highest specific catalytic activity in the HER, which was $\sim$2 times higher than that of the Nafion-Pt/C sample in alkaline solutions. The high mass activity of the C7-SF25-QAF-3.0 binder-Pt/C catalyst offers potential to reduce the Pt loading on the cathode in practical AEMWEs. These findings emphasize the critical role of anionic binders in alkaline HER systems for practical nanoparticle catalysts.

This work was partly supported by the New Energy and Industrial Technology Development Organization (NEDO), the Ministry of Education, Culture, Sports, Science and Technology (MEXT), Japan, through Grants-in-Aid for Scientific Research (23H02058) and MEXT Program: Data Creation and Utilization Type Material Research and Development Project (JPMXP 1122712807), JST (GteX JPMJGX23H2), and JKA promotion funds from KEIRIN RACE.

Data availability

The data supporting this article have been included as part of the ESI.†

Conflicts of interest

There are no conflicts to declare.

Notes and references

1 A. Hassanpouryouzband, M. Wilkinson and R. S. Haszeldine, *Chem. Soc. Rev.*, 2024, **53**, 2258–2263.
2 R. Sang, Z. Wei, Y. Hu, E. Alberico, D. Wei, X. Tian, P. Ryabchuk, A. Spannenberg, R. Razzaq and R. Jackstell, *Nat. Catal.*, 2023, **6**, 543–550.
3 C. Li and J.-B. Baek, *Nat. Energy*, 2021, **87**, 106162.
4 N. Du, C. Roy, R. Peach, M. Turnbull, S. Thiele and C. Bock, *Chem. Rev.*, 2022, **122**, 11830–11895.
5 J. Durst, A. Siebel, C. Simon, F. Hasché, J. Herranz and H. Gasteiger, *Energy Environ. Sci.*, 2014, **7**, 2255–2260.
6 P. Mardle, B. Chen and S. Holdcroft, *ACS Energy Lett.*, 2023, **8**, 3330–3342.
7 J. Fang, G. Zhang, M.-A. Goulet, P. Zuo, Y. Zhou, H. Li, J. Jiang, M. D. Guiver, Z. Yang and T. Xu, *Nat. Commun.*, 2025, **16**, 3282.
8 L. Yin, R. Ren, L. He, W. Zheng, Y. Guo, L. Wang, H. Lee, J. Du, Z. Li and T. Tang, *Angew. Chem., Int. Ed.*, 2024, **63**, e202400764.
9 W. Yu, Y. Xu, Z. Liu, F. Luo, X. Sun, X. Li, F. Duan, X. Liang, L. Wu and T. Xu, *J. Am. Chem. Soc.*, 2024, **146**, 22590–22599.
10 H. Cao, J. Pan, H. Zhu, Z. Sun, B. Wang, J. Zhao and F. Yan, *Adv. Sci.*, 2021, **8**, 2101744.
11 R. Jervis, N. Mansor, A. J. Sobrido, S. Jones, C. Gibbs, T. P. Neville, J. Millichamp, P. R. Shearing and D. J. Brett, *J. Electrochem. Soc.*, 2017, **164**, F1551.
12 J. Wang, Y. Zhao, B. P. Setzler, S. Rojas-Carbonell, C. Ben Yehuda, A. Amel, M. Page, L. Wang, K. Hu and L. Shi, *Nat. Energy*, 2019, **4**, 392–398.
13 N. Chen, S. Y. Paek, J. Y. Lee, J. H. Park, S. Y. Lee and Y. M. Lee, *Energy Environ. Sci.*, 2021, **14**, 6338–6348.
14 H. Ono, T. Kimura, A. Takano, K. Asazawa, J. Miyake, J. Inukai and K. Miyatake, *J. Mater. Chem. A*, 2017, **5**, 24804–24812.
15 F. Liu, K. Miyatake, A. M. A. Mahmoud, V. Yadav, F. Xian, L. Guo, C. Y. Wong, T. Iwataki, Y. Shirase and K. Kakinuma, *Adv. Energy Mater.*, 2024, 2404089.
16 S. Tanaka, S. Takaya, T. Kumeda, N. Hoshi, K. Miyatake and M. Nakamura, *Int. J. Hydrogen Energy*, 2021, **46**, 28078–28086.
17 Y. Zou, K. Miyatake, F. Liu, L. Guo, C. Y. Wong, A. Mohamed Ahmed Mahmoud, V. Yadav and F. Xian, *Macromolecules*, 2024, **57**, 9833–9840.
18 F. Liu, K. Miyatake, M. Tanabe, A. M. A. Mahmoud, V. Yadav, L. Guo, C. Y. Wong, F. Xian, T. Iwataki and M. Uchida, *Adv. Sci.*, 2024, **11**, 2402969.
19 W. Yu, Y. Xu, X. Shen, X. Yang, Z. Liu, H. Wang, X. Liang, X. Ge, M. D. Guiver and L. Wu, *Next Energy*, 2024, **3**, 100104.
20 D. Dru, S. Baranton, J. Bigarre, P. Buvat and C. Coutanceau, *ACS Catal.*, 2016, **6**, 6993–7001.
21 S. J. Paddison and R. Paul, *PCCP*, 2002, **4**, 1158–1163.
22 Y. Garsany, R. W. Atkinson, M. B. Sassin, R. M. Hjelm, B. D. Gould and K. E. Swider-Lyons, *J. Electrochem. Soc.*, 2018, **165**, F381–F391.
23 D. Bresser, D. Buchholz, A. Moretti, A. Varzi and S. Passerini, *Energy Environ. Sci.*, 2018, **11**, 3096–3127.
24 B. Britton and S. Holdcroft, *J. Electrochem. Soc.*, 2016, **163**, F353.
25 J. Xue, J. Zhang, X. Liu, T. Huang, H. Jiang, Y. Yin, Y. Qin and M. D. Guiver, *Electrochem. Energy Rev.*, 2022, 1–53.
26 X. Wu, W. Chen, X. Yan, G. He, J. Wang, Y. Zhang and X. Zhu, *J. Mater. Chem. A*, 2014, **2**, 12222–12231.
27 J. Xue, J. C. Douglin, K. Yassin, T. Huang, H. Jiang, J. Zhang, Y. Yin, D. R. Dekel and M. D. Guiver, *Joule*, 2024, **8**, 1457–1477.